

УДК 532.526.4

UDC 532.526.4

**ТЕОРИЯ ТУРБУЛЕНТНОСТИ И
МОДЕЛИРОВАНИЕ ТУРБУЛЕНТНОГО
ПЕРЕНОСА В АТМОСФЕРЕ
ЧАСТЬ 4**

**THEORY OF TURBULENCE AND
SIMULATION OF TURBULENT TRANSPORT
IN THE ATMOSPHERE
PART 4**

Трунев Александр Петрович
к. ф.-м. н., Ph.D.
Директор, A&E Trounev IT Consulting, Торонто,
Канада

Alexander Trunev
Ph.D.
Director, A&E Trounev IT Consulting, Toronto,
Canada

В работе представлена полностью замкнутая модель турбулентного пограничного слоя, полученная из уравнения Навье-Стокса. Фундаментальные константы пристенной турбулентности, включая постоянную Кармана, определены из теории. Эта модель была развита для ускоренного и неизотермического пограничного слоя над шероховатой поверхностью

The completely closed model of wall turbulence was derived directly from the Navier-Stokes equation. The fundamental constants of wall turbulence including the Karman constant have been calculated within a theory. This model has been developed also for the accelerated and non-isothermal turbulent boundary layer flows over rough surface

Ключевые слова: АТМОСФЕРНАЯ
ТУРБУЛЕНТНОСТЬ, ТУРБУЛЕНТНЫЙ
ПЕРЕНОС, УСКОРЕННЫЕ ТЕЧЕНИЯ,
ПОГРАНИЧНЫЙ СЛОЙ, ШЕРОХОВАТАЯ
ПОВЕРХНОСТЬ, ПРИЗЕМНЫЙ СЛОЙ
АТМОСФЕРЫ, ТУРБУЛЕНТНЫЙ ПЕРЕНОС
АЭРОЗОЛЕЙ

Keywords: ACCELERATED FLOW, AEROSOL
TURBULENT TRANSPORT, ATMOSPHERIC
STRATIFIED FLOW, ATMOSPHERIC
TURBULENCE, ATMOSPHERIC SURFACE
LAYER, BOUNDARY LAYER, ROUGH
SURFACE, TURBULENT TRANSPORT

4. Theory of turbulent flows in temperature and pressure gradients

The problem of turbulent flow in the gravitational field with a prescribed gradient of temperature (problem of stationary atmospheric turbulent convection) has been considered. Generalisation of Monin-Obukhov's theory of similarity [21-22] has been given.

The model of the turbulent boundary layer in pressure gradient has been presented. An application of this model to atmospheric boundary layer, on a scale of which the planet rotation plays an important role has been adopted.

4.1. Thermal boundary layer

The problem of mass and heat-transfer in non-isothermal turbulent boundary layers has been studied by many authors [1, 3-12, 15-115]. In the last three decades numerical methods of calculations of heat-transfer have been successfully developed [51, 116].

Let us consider a model of non-isothermal turbulent boundary layer based on the theory of turbulence considered above. In a case of a steady flow third equation (2.10) can be written as

$$\text{Pr} \frac{\tilde{W}}{h} \frac{\partial T^+}{\partial h} = \frac{n}{h^2} \frac{\partial}{\partial h} (1 + n^2 h^2) \frac{\partial T^+}{\partial h} - \frac{nn^2 h}{h^2} \frac{\partial T^+}{\partial h} \quad (4.1)$$

where $T^+ = (T_g - \tilde{T}) / T_*$, $T_* = q_H / (r c_p u_t)$ is the turbulent scale of tempera-

ture, q_H is the heat flux from the rigid surface to the air, c_p is the specific heat at constant pressure of the gas.

The boundary conditions for equation (4.1) on a smooth wall and for the long distance from the wall are given by

$$\begin{aligned} z^+ = 0: \quad T^+ = 0; \quad dT^+ / dz^+ = \text{Pr} \\ z^+ \rightarrow \infty: \quad dT^+ / dz^+ \rightarrow 1 / k_h z^+, \end{aligned} \quad (4.2)$$

where k_h is a constant which is approximately equal to the Karman constant.

Neglected by the term in the left part of (4.1) in special case when $\text{Pr} \rightarrow 0$ one can derive a general solution of the boundary value problem (4.1)-(4.2) in the form:

$$T^+ = \frac{1}{k_h} \text{Arsh}(k_h \text{Pr} z^+) \quad (4.3)$$

The temperature profile (4.3) well demonstrates that the main turbulent scale of the thermal layer is not the same as the turbulent length scale of the dynamic boundary layer:

$$l_T \approx n / (k_h \text{Pr} u_t) \neq l_0 \approx 8.71n / u_t.$$

Hence in a common case two independent length scales should be defined in the turbulent non-isothermal boundary layer problem.

For the long distance from the wall, $z^+ \gg 1 / k_h \text{Pr}$, the mean temperature profile (4.3) is resulted to the logarithmic profile:

$$T^+ = \frac{1}{k_h} \ln z^+ + c_h(\text{Pr})$$

where $c_h(\text{Pr}) = k_h^{-1} \ln(2k_h \text{Pr})$.

If the Prandtl number is about unit, $\text{Pr} \approx 1$, then the temperature gradient near to the wall essentially depends on the dynamic boundary layer parameters. For this case the temperature gradient in a steady turbulent boundary layer at a given heat flux on the wall can be described by equation (4.1) rewritten in the form:

$$\frac{\tilde{W}_1}{h_1} \frac{\partial T^+}{\partial h_1} = \frac{n}{\text{Pr} h_1^2} \frac{\partial}{\partial h_1} (1 + n_1^2 h_1^2) \frac{\partial T^+}{\partial h_1} - \frac{n n_1^2 h_1}{\text{Pr} h_1^2} \frac{\partial T^+}{\partial h_1} \quad (4.4)$$

where $\tilde{W}_1 = \tilde{w} - h_1 \Phi_1$, $\Phi_1 = h_{1t} + h_{1x} \tilde{u} + h_{1y} \tilde{v}$, $z = h_1(x, y, t)$ is the surface of the thermal sublayer chosen for the turbulence modelling, $h_1 = z / h_1$, $n_1 = \sqrt{h_{1x}^2 + h_{1y}^2}$.

In this problem the universal parameters can be defined as follows

$$x_1 = z / l_T, \quad l_T = h_1 / n_1, \quad a_1 = \arctan(h_{1y} / h_{1x}), \quad w_T^+ = h_{1t} / n_1 u_t,$$

$$\tilde{W}_1 = \tilde{w} - h_1 \Phi_1 = \tilde{w} - x_1 u_t [j \cos(a - a_1) + y \sin(a - a_1) + w_T^+ - w_0^+ \cos(a - a_1)]$$

For atmospheric flows when $Pr \approx 1$ we can suggest that $a_1 = a, w_T^+ = w_0^+$, therefore $\tilde{W}_1 / u_t = (x - x_1)j - c$. Used this nomenclatures and boundary conditions (4.2) one can derived the temperature gradient as a solution of equation (4.4) as follows

$$\frac{dT^+}{dz^+} = \frac{Pr \exp[-Pr I_T^+ I_1 - Pr I_T^+ (1 - \bar{I}) I_2]}{\sqrt{1 + x_1^2}} \tag{4.5}$$

where $I_1 = \int_0^{x_1} \frac{c(\bar{I}x) dx}{1+x^2}$, $I_2 = \int_0^{x_1} \frac{j(\bar{I}x)x dx}{1+x^2}$, $\bar{I} = I_T / I_0$.

Since the problem (4.5) with (4.2) is analogue to that which has been used for the mean velocity profile calculation, thus one can establish the equation connected the constants of turbulence theory which is similar to (2.24), as follows:

$$k_h = w_0^+ \frac{\exp[P_t I_{01}(R_t, \bar{I}) + P_t (1 - \bar{I}) I_{02}(R_t, \bar{I})]}{P_t} \tag{4.6}$$

where $P_t = Pr I_1^+ w_0^+$ is the Peclet number calculated on the thermal sublayer surface parameters,

$$I_{01} = \int_0^\infty \frac{c(\bar{I}x) dx}{1+x^2}, I_{02} = \int_0^\infty \frac{j(\bar{I}x)x dx}{1+x^2}.$$

It should be noted that $\bar{I} = Pr^{-1} P_t / R_t$ and that for $\bar{I} = 1$ equation (4.6) is resulted to (2.24). Thus to define the thermal length scale and parameter k_h with the given $R_t = R_t^*$, the equation (4.6) can be used in the same way as the Karman constant has been calculated: k_h is the constant at small variations of the Peclet number if $dk_h / dP_t = 0$, therefore some critical value $P_t = P_t^*(Pr, R_t^*)$ can be calculated as the root of this equation.

The value $k_h = k_h(Pr)$ computed on this model practically is a constant, $k_h \approx k$ for the range $0.4 \leq Pr \leq 1.5$ - see Figure 4.1. The computed stable mean value of the Peclet number is given by

$$P_t^*(Pr, R_t^*) = R_t^* (1 + 0.217 \ln(Pr))$$

for the Prandtl number in the range $0.1 \leq Pr \leq 2$. The thermal layer length is defined as $I_T^+ = P_t^* / Pr w_0^+ = I_0^+ (1 + 0.217 \ln(Pr)) / Pr$. The mean temperature profiles calculated on (4.5) for various Prandtl number $Pr = 0.2; 0.3; 0.5; 0.7$ can be compared with the model of Cebeci [51] - see Figure 4.2 (right). It's well known that

the Cebeci model based on the turbulent Prandtl number conception and it can be written as follows (see Cebeci & Bradshaw [51]) :

$$\frac{dT^+}{dz^+} = \frac{\text{Pr}}{1 + e_m^+ \text{Pr} / \text{Pr}_t},$$

$$e_m^+ = (kz^+)^2 [1 - \exp(-z^+ / l_d^+)]^2 \frac{du^+}{dz^+}$$

The mean velocity gradient in the right part of the second equation is given by Van Driest model (2.29), Pr_t is the turbulent Prandtl number, l_t is the damping length of the turbulent thermal layer, defined as

$$\text{Pr}_t = \frac{k[1 - \exp(-z^+ / l_d^+)]}{k_h[1 - \exp(-z^+ / l_t^+)]}, \quad l_t^+ = \frac{1}{\sqrt{\text{Pr}}} \sum_{i=1}^5 C_i \lg^{i-1} \text{Pr}$$

Here $C_1 = 34.96; C_2 = 28.79; C_3 = 33.95; C_4 = 6.3; C_5 = -1.186$.

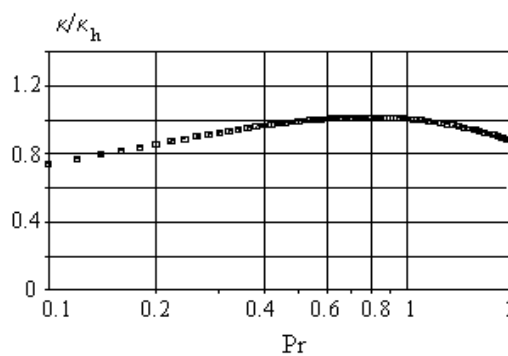


Figure 4.1: The ratio k / k_h versus the molecular Prandtl number

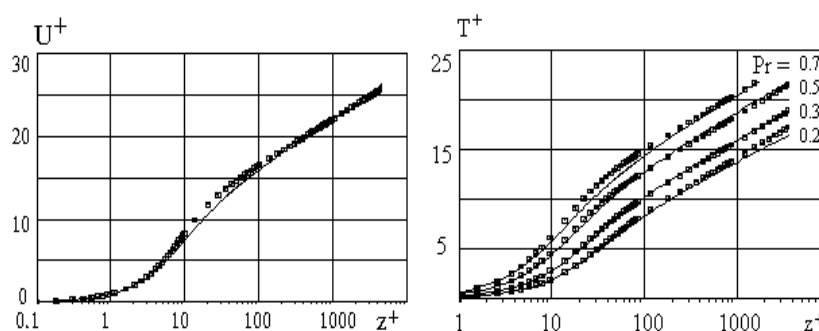


Figure 4.2: Mean velocity (left) and temperature (right) profiles in the turbulent boundary layer computed on the Cebeci model (symbols) and on (4.5) - solid lines

As it is shown in Figure 4.2 the agreement between the predicted profiles and the widely used models of van Driest and Cebeci in general is good. But the present model depends on only one constant, while, for instance, the Cebeci model depends on 8 constants as minimum.

The thermal layer stays closer to a wall than the viscous sublayer for $Pr > 1$ and farther from it for $Pr < 1$ as it follows from the thermal layer length scale, $I_T^+ = I_0^+(1 + 0.217 \ln(Pr)) / Pr$. For the small Prandtl number, $Pr \ll 1$, the thermal sublayer is so thick that completely consists of the viscous sublayer. In the case when $Pr \rightarrow 0$, the thermal layer practically is independent on the dynamic transition layer, and the mean temperature profile is given by equation (4.3) - see Figure 4.3 (left), with thermal length scale $I_T \approx n / (k_h Pr u_t)$.

In another case when $Pr \gg 1$ (practically when $Pr \geq 2$) the thermal sublayer is so thin that it is included in the viscous sublayer as a whole. Figure 2.2 shows that in this case the solutions with the negative quantity of the dynamic roughness parameter $R_t < 0$ effects on the thermal layer near the wall. Suggesting that $a_1 = a, w_T^+ = w_0^+$, and using the expression $\tilde{W}_1 / u_t = w^+(\bar{I} x_1) - x_1 j(\bar{I} x_1)$ the mean temperature gradient (4.5) can be rewritten as follows

$$\frac{dT^+}{dz^+} = \frac{Pr \exp[Pr I_T^+ I_3(x_1, \bar{I}) - Pr I_T^+ I_2(x_1, \bar{I})]}{\sqrt{1+x_1^2}} \tag{4.7}$$

where $I_3 = \int_0^{x_1} \frac{w^+(\bar{I} x) dx}{1+x^2}, I_2 = \int_0^{x_1} \frac{j(\bar{I} x) x dx}{1+x^2}$.

Integrating by parts and using the boundary conditions on the wall: $w^+(0) = 0; j(0) = w_0^+$, the last integrals can be transformed as follows:

$$\int_0^{x_1} \frac{w^+(\bar{I} x) dx}{1+x^2} = w^+(x) \arctan(x_1) - \int_0^{x_1} \frac{dw^+}{dx_1} \arctan(x_1) dx_1 \tag{4.8}$$

$$\int_0^{x_1} \frac{j(\bar{I} x) x dx}{1+x^2} = \frac{1}{2} j(x) \ln(1+x_1^2) - \frac{\bar{I}}{2} \int_0^{x_1} j_x \ln(1+x_1^2) dx_1$$

The third equation (2.16) can be written in the form

$$\frac{dw^+}{dx} = x \frac{dj}{dx} = \frac{w_0^+ a x e^{-I}}{1+x^2}$$

Using this equation and secondary integrating by parts the integrals in the right side of (4.8) we have:

$$\int_0^{x_1} \frac{dw^+}{dx_1} \arctan(x_1) dx_1 = \bar{I} \int_0^{x_1} \frac{dw^+}{dx} [\arctan(x_1) - p/2] dx_1 + \frac{p}{2} w^+$$

If $Pr \gg 1$, then $\bar{I} \approx I_0^+ Pr^{-1} \ll 1$, therefore we can estimate the contributions of all terms versus the small parameter, $\bar{I} \ll 1$, as follows:

$$\bar{I} \int_0^{x_1} \frac{dw^+}{dx} [\arctan(x_1) - p/2] dx_1 = \bar{I}^2 \int_0^{x_1} \frac{w_0^+ a x_1 e^{-I}}{1+x^2} [\arctan x_1 - p/2] dx_1$$

The last expression is proportional to \bar{I}^2 for $x_1 \leq 1$, and to \bar{I} for $x_1 \rightarrow \infty$. Therefore the first integral (4.8) can be estimated as

$$\int_0^{x_1} \frac{w^+ (\bar{I} x) dx}{1+x^2} = w^+(x) (\arctan x_1 - p/2) + O(\bar{I})$$

The function in the right part of the last expression is proportional to \bar{I}^2 , because in the wall region the normal velocity is about $w^+ \approx 0.5 w_{xx}^+(0) (\bar{I} x_1)^2$. Hence as it follows from above, for the large quantity of the Prandtl number the mean temperature profile depends on the normal velocity as a weak function which is proportional to \bar{I}^2 for $x_1 \leq 1$ and to \bar{I} for $x_1 \rightarrow \infty$.

Using this result it is possible to derive a simple equation for the mean temperature gradient, which is satisfactory agreed with experimental data in a wide range of the Prandtl number. Integrating by parts the term in the right part of second equation (4.8), we have

$$\int_0^{x_1} j_x \ln(1+x_1^2) dx_1 = j_x J(x_1) - \bar{I} \int_0^{x_1} j_{xx} J(x_1) dx_1$$

where $J(x_1) = x_1 \ln(1+x_1^2) - 2x_1 + 2 \arctan x_1$. This process can be prolonged and the formal series in powers of \bar{I} can be found. The first and second terms of this series are equal to zero on the wall and for $x_1 \rightarrow \infty$. Hence, the equation, connecting constants of the theory, similar to (4.5), has in this case a very simple form: $I_T^+ = 1/k_h Pr$, that coincides with the thermal layer length scale specified above for $Pr \ll 1$.

Substituting the derived expressions in equation (4.7) and using the first term of the series one can write the mean temperature gradient as

$$\frac{dT^+}{dz^+} = \frac{Pr \exp[-0.5 P j_1(x) \ln(1+x_1^2)]}{\sqrt{1+x_1^2}} \tag{4.9}$$

where $j_1 = dc_1/dx$ is given by (2.19).

The equation (4.9) contains the free parameter $P_t = w_0^+ I_T^+ Pr$, which is the Peclet number. As it was established in the numerical experiments, to agree (4.9), for example, with the model of Cebeci [51], it is enough to consider this parameter as a function, which depends on the Prandtl number. The numerically approximated function, $P_t(Pr)$, is given by $P_t = -1.61 / (1 + 0.1 \ln Pr)$ in the range of the Prandtl number from 2 up to 10^3 . Hence, the Peclet number is the negative quantity. In turn it means that $w_0^+ < 0$. Therefore the mean temperature profile depends mainly on the dynamic roughness surface disturbances, which move to the wall for $w_0^+ < 0$. The mean temperature profiles computed on equation (4.9) are shown in Figure 4.3 (right) by solid lines together with the profiles computed on the model of Sebeci [51] - the symbolized lines. The agreement between two models in general is good.

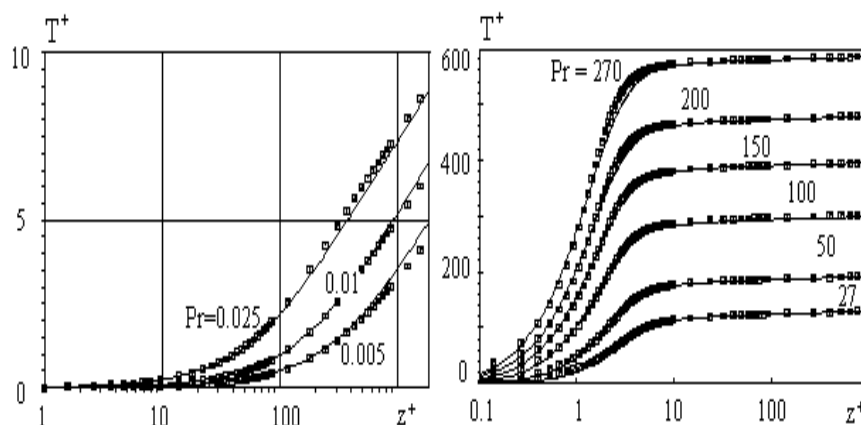


Figure 4.3: Mean temperature profiles in the turbulent boundary layer computed for the small (left) and large Prandtl numbers (right) on the model of Sebeci [51] - symbols, and on the proposed model - solid lines

The mean temperature profiles computed on the model (4.9) are well correlated with the model of Sebeci also for $Pr \leq 1$, because the parameter $\bar{I} = 1 / (k_h Pr I_0^+)$ is the small quantity even for $Pr \approx 1$.

This theory can be formulated shortly, using the transformation formula for $I_3 - I_2$ in (4.7) as follows

$$\int_0^{x_1} \frac{[w^+(\bar{I}x)/x - j(\bar{I}x)]x dx}{1+x^2} = \frac{1}{2} [w^+(x)/x_1 - j(x)] \ln(1+x_1^2) - \frac{\bar{I}(\bar{I}-1)}{2} \int_0^{x_1} j_x \ln(1+x^2) dx + \int_0^{x_1} \frac{w^+(\bar{I}x)}{x^2} \ln(1+x^2) dx$$

Then substituted the approximation of the normal velocity near the wall, $w^+ \approx 0.5w_{xx}^+(0)(\bar{I}x_1)^2$, in the right part of the last expression, finally we have

$$I_3 - I_2 = -\frac{1}{2}j(x) \ln(1+x_1^2) - \frac{\bar{I}(\bar{I}-1)}{2} \int_0^{x_1} j_x \ln(1+x^2) dx + O(\bar{I}^2)$$

Obviously that this approximation is relatively good for $\bar{I} \rightarrow 0$ as well as for $\bar{I} \approx 1$. Since the equation (4.9) is based on this approximation, it can be established that the normal velocity contribution in the mean temperature profile is a relatively small value (this contribution depends on the second derivation of the normal velocity on the wall which is estimated for the mean flow as $w_{xx}^+(0) = j_x(0) = w_0^+ a \approx -0.127$). From the data shown in Figure 2.8 one can conclude that the turbulence intensity normal velocity profile has a maximum for $z^+ \approx 50$ where the mean temperature profile - see Figure 4.3 (right), is described by a logarithmic function. Thus as it follows from equation (4.9) the interaction of the temperature and velocity fluctuations for the large Prandtl number primarily depends on the function $j(x)$ which is proportional to the dynamic roughness parameters, i.e., $j = u^+ \cos a + v^+ \sin a + w_0^+$.

In the mixed layer the common expression of the mean temperature profile is given by

$$T^+ = e_T T_{in}^+(z^+) - \frac{e_T}{k_h} (\text{Arsh}(\bar{z}) + \text{Arsh}(\bar{z}_0)) \tag{4.10}$$

where $e_T = 1 / (1 - 1 / k_h V_* \text{Re}_* \sqrt{1 + \bar{z}_0^2})$, T_{in}^+ is the mean temperature profile in the inner layer.

As it has been established the mean temperature profile in the outer region of the turbulent boundary layer depends on two parameters: $z_0 = 0.5H_{th}$ and $V_* \approx 2$. But the thermal layer scale in the outer region is not equal to the dynamic layer scale $H_{th} \neq H$.

Apparently, that model (4.9) seems to be more simplified then (4.7). Nevertheless the model (4.7) is preferable for the theoretical consideration because using this model it is possible to calculate the Peclet number as function of the Prandtl number, $P_t(\text{Pr})$, without any experimental data.

4.2 Turbulent flow in the stratified surface layer

Usually the atmospheric boundary layer has a thermal stratification in the bottom part due to the solar radiation and the heat-transfer from the ground surface to the air. In common case the temperature stratification produces some dynamic effect in the air flow such the local free convection due to buoyancy forces. The consideration of this problem based on the similarity theory was given by Monin & Obuchov [21]. The main parameter of the Monin & Obuchov theory is the length scale

$$L = -u_*^3 r c_p T_0 / (k g q_H)$$

where T_0 is the air temperature in the surface layer, q_H is the heat flux from the ground to the air.

As it was established (see [21-22]) for $L > 0$ the stratified layer is stable, at $L < 0$ is unstable, for $L \rightarrow \infty$ neutral stratification is attained what means that there is no thermal effect on the turbulent flow. Let us consider the Monin & Obuchov theory based on the present theory of turbulence.

The introduced parameter B in the right part of the second equation (2.12) is connected with the length scale L introduced by Monin & Obuchov [21-22] as follows

$$B = n / (u_* k L)$$

Therefore, the stable flows are realized for $B > 0$, the unstable flows - for $B < 0$, and the neutral stratified flows for $B = 0$. Thus to estimate the turbulent stratified flow parameters based on the present theory of turbulence we should establish the boundary conditions and the theoretical constants (or the parameters with stars). The proposed model can be written as

$$\frac{dc}{dx} = j, \tag{4.11}$$

$$(1+x^2) \frac{d^2j}{dx^2} + (I_0^+ c + 2x) \frac{dj}{dx} = -B_0 \frac{x I_0^{+2} T^+}{1+x^2}$$

$$\frac{du^+}{dz^+} = \frac{e^{-I}}{\sqrt{1+(z^+ / I_0^+)^2}},$$

$$\frac{dT^+}{dz^+} = \frac{\text{Pr} \exp[-\text{Pr} I_T^+ I_1 - \text{Pr} I_T^+ (1 - \bar{I}) I_2]}{\sqrt{1+(z^+ / I_T^+)^2}}$$

where $I_T^+ = I_0^+ (1 + 0.217 \ln \text{Pr}) / \text{Pr}$, $x = z^+ / I_0^+$, $x_1 = z^+ / I_T^+$;

$$I = \int_0^x \frac{I_0^+ c dx}{1+x^2}, I_1 = \int_0^{x_1} \frac{c(\bar{I} x) dx}{1+x^2}, I_2 = \int_0^{x_1} \frac{j(\bar{I} x) x dx}{1+x^2}.$$

As it has been established the buoyancy force parameter depends on the type of stratification as a discontinuous function

$$B_0 = \begin{cases} B, & L < 0 \\ 41.85B, & L > 0 \end{cases}$$

This dependence can be explained by the influence of the large scale random amplitudes with $I^+ = 30.24$ (a maximal root of the equation $k = w_0^+ \frac{\exp[I_0(R_t)]}{R_t}$ for $k = 0.41$) on the mean velocity profile in a case of the stable stratification. It can

be shown that the buoyancy force term in the right part of the second equation (2.12) increases as third degree of the ratio of two scales, i.e. as $(I^+ / I_0^+)^3 \approx 41.85$.

The boundary condition for equation system (4.11) on the imaginary smooth surface is given by

$$x = 0: \quad c(0) = T^+(0) = u^+(0) = 0, \quad j(0) = w_0^+ \quad (4.11, a)$$

In the outer region in a case of unstable stratification the boundary conditions can be established for $z^+ \rightarrow \infty$ as follows

$$\lim_{z^+ \rightarrow \infty} u^+(z^+) = u_\infty^+(B), \quad \lim_{z^+ \rightarrow \infty} T^+(z^+) = T_\infty^+(B) \quad (4.11, b)$$

where parameters $u_\infty^+(B), T_\infty^+(B)$ can be deduced from the experimental data.

In a case of a stable stratification the boundary conditions can be formulated at the level $z = L$:

$$u^+ = u^+(L), \quad T^+ = T^+(L) \quad (4.11, c)$$

where the given values $u^+(L), T^+(L)$ also can be defined by the empirical way.

The mean velocity and temperature profiles in the stable and unstable turbulent flows, computed on the present model (4.11), are shown in Figures 4.4 and 4.5 (solid lines 2). For a comparison in these Figures the profiles computed on the Monin-Obuchov model [21-22] are shown by the broken lines 1. It is a well known fact (see, for instance, [23-24, 26-27, 117-119]) that this model can be formulated for the mean velocity and temperature gradient as follows

$$\frac{\partial u^+}{\partial z^+} = \frac{f_m(z/L)}{kz^+}, \quad \frac{\partial T^+}{\partial z^+} = \frac{f_h(z/L)}{kz^+} \quad (4.12)$$

The momentum and heat universal functions f_m, f_h have been established several times from experimental data by Businger *et al* [23], Dyer [26], Van Ulden & Holtslag [27], Hogstrom [117], Beljaars & Holtslag [118] and other.

For the Karman constant $k = 0.41$ the universal functions have been estimated by Pugliese *et al* [119] in the form

$$f_m = \begin{cases} (1 - 20.6z/L)^{-1/4}, & L < 0 \\ 1 + 6.45z/L, & L > 0 \end{cases} \quad (4.13)$$

$$f_h = \begin{cases} 1.015(1 - 12.35z/L)^{-1/2}, & L < 0 \\ 1.015 + 8.35z/L, & L > 0 \end{cases}$$

To agree the mean velocity and temperature profiles computed on the models (4.11) and (4.12) for $z^+ \rightarrow 0$ the model (4.12) has been regularised at $z^+ \rightarrow 0$ as follows

$$\frac{\partial u^+}{\partial z^+} = \frac{f_m(z/L)}{kI_0^+ \sqrt{1+(z^+/I_0^+)^2}}, \quad \frac{\partial T^+}{\partial z^+} = \frac{f_h(z/L)}{kI_0^+ \sqrt{1+(z^+/I_0^+)^2}} \quad (4.14)$$

The boundary conditions on the imaginary smooth wall for this equation system can be given as

$$T^+(0) = \begin{cases} 6.5, & L < 0 \\ 6, & L > 0 \end{cases}, \quad u^+(0) = \begin{cases} 8.5, & L < 0 \\ 8.5, & L > 0 \end{cases} \quad (4.14')$$

The boundary conditions are chosen here in the form (4.14') since the model (4.12) with universal functions (4.13) describes actually the turbulent flow over a rough surface, and the model (4.11) has been formulated for the turbulent flow over a smooth surface. To derive these conditions, note that the mean velocity shift in the neutral stratified turbulent flow over rough surface given by equation (3.2) can also be used for the stratified flows.

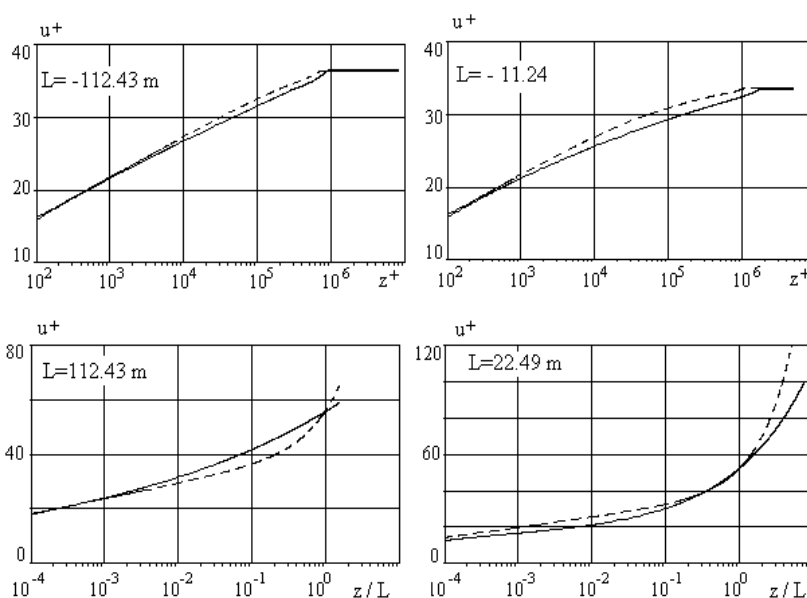


Figure 4.4: The mean velocity profiles in the stratified surface layer computed on (4.11) - the solid lines, and (4.14) - the broken lines

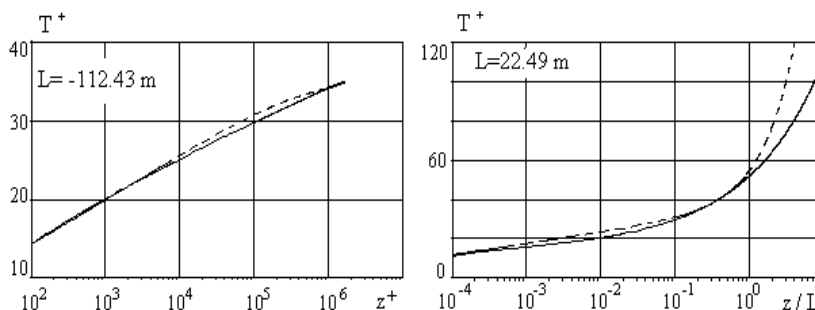


Figure 4.5: The mean temperature profiles in the unstable (left) and stable (right) turbulent boundary layers computed on (4.11) - the solid lines, and (4.14) - the broken lines

As it follows from the data shown in Figures 4.4-4.5 in a case of an unstable stratification ($L=-112.43$ m, $L=-11.24$ m) the agreement between two models (4.11) and (4.14) in general is good for the mean velocity profile as well as for the mean temperature. In a case of a stable stratification ($L=112.43$ m, $L=22.49$ m) the profiles computed on two models are agreed only for $z \leq L$ and then the profiles diverge one from another. These outcomes can be explained with the next simple model. Put the new variable $V = I \operatorname{Arsh}(z/I)$ in the third equation (1.14) normalised as $y = \Psi / nu_*$, and then it can be rewritten as

$$\frac{\tilde{W}}{\operatorname{ch}(V/I)} \frac{\partial y}{\partial V} = n \frac{\partial^2 y}{\partial V^2}.$$

Using the approximate formula $W^+ \approx W_0^+(x_0) - w_0^+ j_0(x - x_0)$, where $j_0 = \lim_{x \rightarrow \infty} j_1(x)$, which can be realised at a large distance from the wall (as it has been established in numerical experiments it can be for $x \geq x_0 \approx 10^2$), one can transformed this equation to the form

$$\Delta W \frac{\partial y}{\partial V} = n \frac{\partial^2 y}{\partial V^2},$$

where $\Delta W = -w_0 j_0(B)$. Put $y = u^+$ for the mean flow, then integrating the derived equation we have

$$\frac{\partial u^+}{\partial V} = \frac{\partial u^+}{\partial V}(V_0) \exp\left[\frac{\Delta W}{n}(V - V_0)\right],$$

$$u^+ = u^+(V_0) + \frac{n}{\Delta W} \frac{\partial u^+}{\partial V}(V_0) [\exp[\Delta W(V - V_0)/n] - 1],$$

where $V_0 = I \operatorname{Arsh}(z_0/I) \approx I \ln(2z_0/I)$.

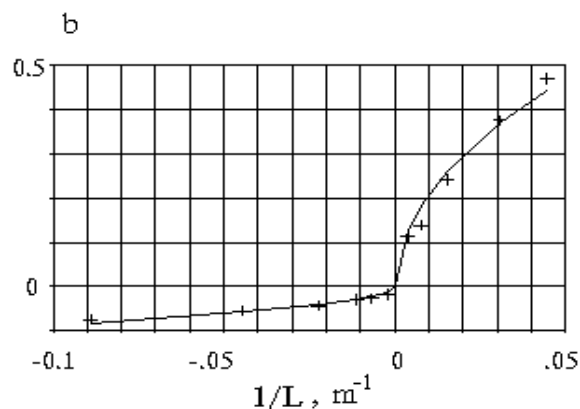


Figure 4.6: The exponent b of the mean velocity profile in the stratified turbulent boundary layer versus the stability parameter $1/L$. The symbols were obtained in the numerical experiments; the solid line is calculated on (4.16)

Using the asymptotic formula $V = I \operatorname{Arsh}(z/I) \approx I \ln(2z/I)$ for $z \gg I$, and put $b = \Delta W l_0 / n$, the last equation can be written as follows

$$u^+ = u^+(z_0^+) + \frac{z_0^+}{b} \frac{\partial u^+}{\partial z^+}(z_0^+) [(z^+ / z_0^+)^b - 1] \quad (4.15)$$

But the mean velocity profile is described by logarithmic function for $z \leq z_0$ therefore for $z > z_0$ we have

$$u^+ = u_0^+ + [(z^+ / z_0^+)^b - 1] / k b$$

where $u_0^+ = k^{-1} \ln(z_0^+) + c$.

As it has been reported by Lui & Kotoda [120] the typical value of the exponent in the velocity profile (4.15) varies for the atmospheric surface layer from $b = -0.1$ for the unstable stratification up to $b = 0.2$ for the stable stratified flows. This is in a good agreement with the numerical data - see Figure 4.6. The numerical data shown in Figure 4.6 can be approximated as follows

$$b(B) = \begin{cases} -24.8(-B)^{\frac{1}{2}}, & L < 0 \\ 173.6B^{\frac{1}{2}}, & L > 0 \end{cases} \quad (4.16)$$

In a case of stable stratification $b > 0$, thus the mean velocity profile increases with the distance from the ground surface as a power function with exponent dependent on the stability parameter accordingly to (4.16). In a case of unstable stratification $b < 0$, hence the mean velocity decreases with the distance as a power function. In a case when $b \rightarrow 0$ the mean velocity profile is resulted to the logarithmic function, that is connected with a neutral stratified flow.

This can be proved also for the mean temperature profile which can be described for $z^+ \geq z_0^+$ by a power function

$$T^+ = T_0^+ + [(z^+ / z_0^+)^{b_1} - 1] / k_h b_1$$

where $b_1 = \operatorname{Pr} \Delta W l_T / n$, $T_0^+ = T^+(z_0^+)$, and $z_0^+ \approx 10^3$.

4.3. Turbulent boundary layer in pressure gradients

The boundary layer can be characterized by a velocity distribution on the upper bound of the turbulent flow, which is connected to a pressure gradient by virtue of the Bernoulli theorem:

$$r U_0 \frac{\partial U_0}{\partial x} = - \frac{\partial p}{\partial x}. \quad (4.17)$$

Though on the boundary of a turbulent layer acceleration and pressure gradient are connected, nevertheless inside a layer this connection is upset. In a

fluid flow the pressure depends on the force affixed to a chosen surface. Therefore, if pressure is affixed on the bound of a boundary layer, it does not completely mean, as the layer as a whole is under effect of this force. The acceleration is connected with a volumetric force, applied to the unit of volume. Therefore the turbulent boundary layer as a whole can be characterized by the external acceleration, that follows immediately from the principle of relativity. Nevertheless, in the literature [121-124] and other the nomenclature has already been taken in connection with the description of turbulent boundary layers in favourable and adverse pressure gradients. So, we will use this nomenclature in a sense, determined by equation (4.17).

Let us consider the problem about an accelerated turbulent flow in the boundary layer with a mean acceleration defined as

$$\left\langle \frac{du}{dt} \right\rangle = a_m U_0 \frac{\partial U_0}{\partial x} \neq 0$$

where a_m is the constant which can be estimated from the experimental data. The equation system for the mean flow in the turbulent boundary layer in pressure gradient can be derived directly from (2.10). Put $a = p/2, y = u^+$ in this equation, and then we have

$$\frac{dc}{dx} = j \tag{4.18}$$

$$(1+x^2) \frac{d^2j}{dx^2} + (I^+c+2x) \frac{dj}{dx} = 0, \quad (1+x^2) \frac{d^2u^+}{dx^2} + (I^+c+x) \frac{du^+}{dx} = I^+g^+$$

where $g^+ = \frac{I^+n}{u_*^3} a_m U_0 \frac{\partial U_0}{\partial x}$ is the dimensionless acceleration parameter.

The non-linear subsystem included first and second equation (4.18) is independent on the streamwise mean acceleration. Thus it can be supplemented by the boundary conditions in the form (2.20) to integrate this subsystem. Substituting the non-linear subsystem solution in the third equation (4.18) we can write the first integral of this equation as follows

$$\frac{du^+}{dx} = \frac{Ce^{-I}}{\sqrt{1+x^2}}, \quad C = I^+ + \int_0^x \frac{I^+g^+e^{I'}}{\sqrt{1+x^2}} dx \tag{4.19}$$

Here $I = I(x)$ is the integral computed as in the case of the turbulent flow in a zero pressure gradient:

$$I(x, R_t) = \int_0^x \frac{R_t c_1(x, R_t) dx}{1+x^2}$$

Here c_1 is the solution of the problem (2.19)-(2.20).

Note, that the integral term in the right part of the second equation (4.19) can be transformed as follows

$$\int_0^x \frac{I^+ g^+ e^I dx}{\sqrt{1+x^2}} = I^+ g^+ e^{I_0} \text{Arsh}(x) + \int_0^x \frac{I^+ g^+ (e^I - e^{I_0}) dx}{\sqrt{1+x^2}}$$

This integral diverges as the logarithmic function at $x \rightarrow \infty$, since $\text{Arsh}(x) \cong \ln(2x)$ for $x \gg 1$. It means that the acceleration effects on the turbulent flow in the outer region more intensively then in the inner layer. In the normal turbulent boundary layer (far away from the verge of separation) the acceleration parameter is a small quantity, i.e., $|g^+| \ll 1$. In this case, the inner layer is formed under the same conditions, as in a zero pressure gradient flow.

Using the inner layer variables, the acceleration parameter, and mixed layer parameters, we propose the mean velocity gradient in the turbulent decelerating flows as follows

$$\begin{aligned} \frac{du^+}{dz^+} = & \frac{e_0 \exp(I_0 - I)}{kI_0^+ \sqrt{1+x^2}} + \frac{I_0^+ g_*^+ e^{-I}}{\sqrt{1+x^2}} \int_0^x \frac{e^I dx}{\sqrt{1+x^2}} - \\ & - \frac{e_0}{kV_* \text{Re}_* \sqrt{1+\bar{z}^2}} + \frac{e\sqrt{1+\bar{z}_0^2}}{kV_* \text{Re}_*(1+\bar{z}^2)} \end{aligned} \quad (4.20)$$

As it has been established in numerical experiments, the acceleration parameter with star is given by

$$g_*^+ = \frac{n}{ku_*^3} U_0 \frac{\partial U_0}{\partial x}, \quad a_m = 1/kI_0^+ \approx 0.28$$

Hence the acceleration length scale parameter is proportional to the scale of viscous sublayer $I^+ \approx 1/k$. Apparently it means that the main part of a power of the supplied pressure gradient is dissipated in the viscous sublayer closed to the wall, and not in the transition layer where $I^+ \approx I_0^+$.

The mean velocity profile as a solution of the equation (4.20) depends on the parameter e , which can be estimated from the comparison with the experimental data - see Figure 4.7. The data base by Nagano *et al* [67-68] has been used to calculate the mean velocity profiles in the turbulent boundary layers in adverse pressure gradients. The estimated profiles are shown in Figure 4.7. The input data and the numerical parameter $e = e(p^+)$ for these profiles are listed in the Table 4.1. The parameters of the mean velocity profile in the turbulent boundary layer in zero pressure gradient are given by

$$k = 0.41; I_0^+ = 8.71; R_t^* = 1.22; z_0 = 0.5H; V_* = 0.27.$$

The agreement between the predicted mean velocity profile (4.20) and the experimental data by Nagano *et al* [67-68] in general is good.

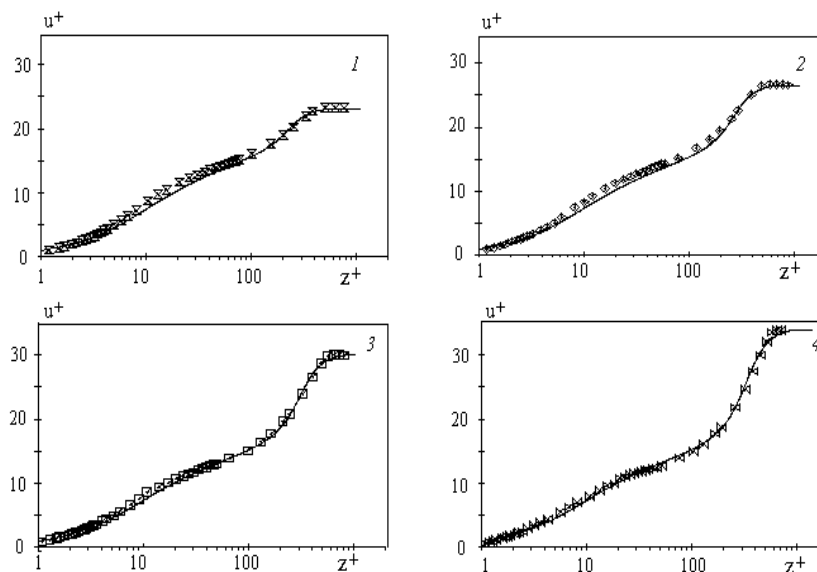


Figure 4.7: The mean velocity profiles in the turbulent boundary layer in adverse pressure gradients computed on (4.20) - the solid lines and experimental data from the data base by Nagano *et al* [68]

The parameter of the mean velocity profile (4.20) increases with the dimensionless pressure gradient parameter, $p^+ = \frac{n}{u_*^3} \frac{\partial p}{\partial x}$, in a case of adverse pressure gradient - see Figure 4.8. This function, $e = e(p^+)$, can be approximated by a cubic polynomial (the trend line in Figure 4.8):

$$e(p^+) \cong 118099p^{+3} - 2386.8p^{+2} + 36.579p^+ + 0.7881.$$

In a case of strong deceleration the turbulent boundary layer depth grows up to the verge of separation (see chapter 6). Opposite, the accelerated turbulent boundary layer becomes thinner and, eventually, the transition to the laminar flow can happen [124].

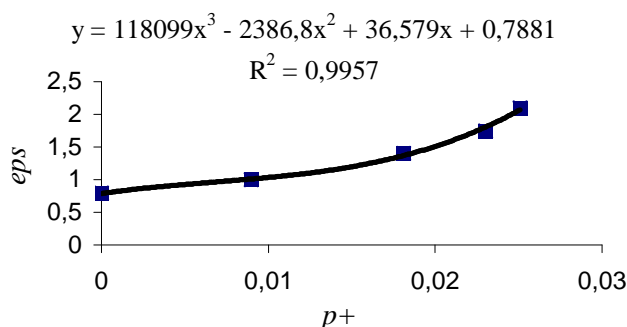


Figure 4.8: The calculated mean velocity profile parameter $e = e(p^+)$ versus the pressure gradient parameter. The equation of the trend line is shown in the bottom part

Table 4.1. The input data for the mean velocity profile (4.20)

| Parameter | The cinematic viscosity $\nu \cdot 10^5$, m^2/s | The friction velocity u_τ , m/s | The boundary layer depth H_{99} , mm | The pressure gradient parameter p^+ | The mean velocity profile parameter ϵ |
|-----------|--|---|---|--|---|
| Figure | | | | | |
| 1.7, b | 1.574 | 0.481 | 13.3 | 0 | 0.79 |
| 3.7.1 | 1.536 | 0.39 | 16.2 | 0.00898 | 1.0 |
| 3.7.2 | 1.576 | 0.307 | 24.6 | 0.0181 | 1.4 |
| 3.7.3 | 1.551 | 0.251 | 34.2 | 0.023 | 1.75 |
| 3.7.4 | 1.537 | 0.197 | 46.1 | 0.0251 | 2.1 |

Thus, the range of feasibility of the model (4.20) depends on this two physical phenomena. It is clear, that model (4.20) cannot be used without the essential modification in the case of the significant acceleration of the turbulent flow.

Nevertheless in the investigated range of parameters model (4.20) can be agreed well with known experimental data, and some results can be explained with this model. For instance, as it was repeatedly underlined by the authors [67-68], the mean velocity profile in the logarithmic layer in adverse pressure gradients passes lower, than in the turbulent flow in a zero pressure gradient. This outcome immediately follows from the equation (4.19), which can be presented as

$$\frac{du^+}{dz^+} = \frac{1 + g^+ I_4(x)}{kz^+}, \quad I_4 = \int_0^x \frac{e^l dx}{\sqrt{1+x^2}} \tag{4.21}$$

Analysing this equation one can conclude that for the turbulent boundary layer in adverse pressure gradient, when $g^+ < 0$, the non-dimensional mean velocity gradient has a less value then in a zero pressure gradient. In a case of favourable pressure gradients, when $g^+ > 0$, the non-dimensional mean velocity gradient has more high value then for a zero pressure gradient flow.

The physical realisation of the accelerated turbulent boundary layers, as it has been explained by Kline *et al* [70], usually is connected with flows in the convergent channels, around cylinder, in a throat nozzle, etc. In these cases the flow geometry affects on the turbulent boundary layer parameters as well as the flow acceleration. It means that in the second equation (4.18) can be added some term described the inertial forces acting in the normal to the wall direction, like the buoyancy forces term in the right part of the second equation (4.11).

The mean velocity profile (4.20) can be regularised in the mixed layer as follows (see [47]):

$$u^+ = u_1^+(z^+) - \frac{I_0^+ g_*^+}{2} (\text{Arsh}^2(\bar{z}) - \text{Arsh}^2(\bar{z}_0)) \tag{4.22}$$

where u_1^+ is given by equation (4.20). As it has been established the estimated free parameter $e = e(p^+)$ is independent on this regularisation.

The turbulent boundary layer in adverse pressure gradient develops up to the verge of separation. Close to the verge of separation the skin friction coefficient decreases down to zero. Due to the strong deceleration the back flow is formed in the wall region. The back flow is characterized by the extremely low Reynolds stresses. The logarithmic layer thickness decreases monotonically up to the verge of separation, thus the turbulent separated flow mainly is similar to the mixed layer. The streamwise velocity pulsation profile in the turbulent separated flow has a maximum in the middle part of the mixed layer while in the turbulent flow with the logarithmic layer the maximum of the streamwise turbulent intensity profile situates near the wall (see Figure 2.6). Using the equation system (2.16) the mean velocity profile in the turbulent separated flow can be modelled as well as in the normal turbulent flow.

4.4. Planetary boundary layer

One of examples of the theory of turbulence application is the atmospheric boundary layer, which is under effect of a pressure gradient and inertial forces, stipulated by rotation of a planet. It is usually supposed, that in the external flow these forces are counterbalanced, therefore the geostrophic flow is formed, which is described by equation

$$r2\Omega_z[\mathbf{e}_z \times \mathbf{U}_0] + \nabla p = 0. \quad (4.23)$$

where $\Omega_z = \Omega \sin j_e$, Ω is the earth's rotation rate, j_e is the latitude, \mathbf{e}_z is the unit vector in OZ direction, $\mathbf{U}_0 = (U_x, U_y)$ is the geostrophic velocity vector.

Hence, in this case it is possible to consider, that the boundary layer is formed under influence of the mean acceleration

$$\left\langle \frac{d\mathbf{u}}{dt} \right\rangle = 2a_m \Omega_z [\mathbf{e}_z \times \mathbf{U}_0] .$$

The non-dimensional acceleration parameters are given by

$$g_x^+ = -\frac{1a_m}{u_*^2} 2\Omega_z U_0 \sin a_0, \quad g_y^+ = \frac{1a_m}{u_*^2} 2\Omega_z U_0 \cos a_0$$

where a_0 is the geostrophical wind angle.

Since the atmospheric boundary layer includes the surface layer and the mixed layer, thus the mean velocity profile can be written as a sum of two terms described the turbulent flow in the bottom and top part of the boundary layer. The main model of the rotating flow with arbitrary stratification in the bottom layer is proposed as

$$\frac{du^+}{dz^+} = \frac{1 + g_x^+ I_4(x)}{e^{I(B)} \sqrt{1+x^2}}, \quad I_4 = \int_0^x \frac{e^{I(B)} dx}{\sqrt{1+x^2}} \quad (4.24)$$

Here $I(B)$ is a function of the stability parameter computed on the base of model (4.11). Note that the model (4.24) is a generalised form of equation (4.19). The mean velocity profile as a combination of two terms can be written by analogue to the mean velocity profile in pressure gradient, see (4.22):

$$U_x = u_t u^+ + \frac{U_0 \cos a_0 - u_t u_\infty^+}{p/2 + \arctan \bar{z}_0} (\arctan \bar{z} + \arctan \bar{z}_0) \quad (4.25)$$

$$u^+ = \frac{1}{k} \ln \frac{z}{r} + c_r + \frac{I_0^+ g_x^+}{2} \ln^2 \frac{z}{r} - \frac{S}{k} (\text{Arsh} \bar{z} + \text{Arsh} \bar{z}_0) - \frac{I_0^+ g_x^+}{2} (\text{Arsh}^2 \bar{z} - \text{Arsh}^2 \bar{z}_0)$$

where $u_\infty^+ = \lim_{z \rightarrow \infty} u^+$, $S = 1 + k I_0^+ g_x^+$, $c_r \approx -6$ is the roughness layer constant. To test this model the velocity profile (4.25) has been compared with the Leipzig data presented by Detering & Etling [125] and used also by Apsley & Castro [44]. The input data for the wind profile and the constants of model are put as follows:

- 1) $a_0 = 26.1^\circ$, $u_t = 0.65 \text{ms}^{-1}$, $H \approx 900 \text{m}$, $r = 0.3 \text{m}$, $U_0 = 17.5 \text{ms}^{-1}$;
- 2) $k = 0.41$, $I_0^+ = 8.71$, $g_x^+ = 0.037$, $z_0 = H$, $V_* = 0.27$.

In the first position the input data, and in the second position the estimated theoretical constants are given. The mean position of the mixed layer is not equal to this value for the turbulent boundary layer on the flat plate. The estimated acceleration parameter, $g_x^+ \approx 0.037$, can be used to calculate the characteristic length scale as

$$l a_m = g^+ u_t^2 / f U_0 \sin a_0 \approx 18 \text{m}$$

where $f = 2\Omega_z \approx 1.13 \cdot 10^{-4} \text{ s}^{-1}$ is the Coriolis parameter (for the Leipzig data). This value can be compared with the maximal mixing length estimated for the Leipzig data by Apsley & Castro [44] as $l_{\max} \approx 36 \text{m}$. Hence, if $l \approx l_{\max} \approx 36 \text{m}$, then $a_m = 0.5$.

The transversal component of the flow velocity in the atmospheric boundary layer remains minor up to height about $0.1H$, and then increases. The velocity vector is turned to the right side counting from the local flow direction. To estimate the transversal velocity gradient the experimental Leipzig data shown in Figure 4.9 can be used. As it follows from this data the turning angle depends on the height approximately as a linear function, $\bar{a} = a_0 z / H$. Using the equation

connected the turning angle and the wind velocity components, $v^+ = u^+ \tan \bar{a}$, one can derive the transversal velocity gradient as:

$$\frac{d v^+}{d z^+} = \frac{d u^+}{d z^+} \tan(a_0 z^+ / \text{Re}_*) + \frac{a_0 u^+}{\text{Re}_* \cos^2 a}$$

In the logarithmic layer this equation has a simple form:

$$\frac{d v^+}{d z^+} = \frac{a_0}{k \text{Re}_*} + \frac{a_0 u^+}{\text{Re}_*}$$

The normal depth of the atmospheric surface layer is about 1 km, hence the dynamic Reynolds number can be estimated as $\text{Re}_* \geq 10^7$. Therefore, the transversal velocity gradient has a small value, which can be neglected in the inner layer.

Thus the wind velocity vector is turned primary in the mixed layer under the pressure gradient effect. Due to this the solution for the transversal velocity profile can be written as follows

$$U_y = u_t v^+ + \frac{U_0 \sin a_0 - u_t v_\infty^+}{p / 2 + \arctan \bar{z}_0} (\arctan \bar{z} + \arctan \bar{z}_0) \quad (4.26)$$

$$v^+ = -\frac{I_0^+ g_y^+}{2} (\arctan^2 \bar{z} - \arctan^2 \bar{z}_0),$$

where $v_\infty^+ = \lim_{z \rightarrow \infty} v^+$. As it has been established the mixed layer parameters in the expression (4.26) is the same as for the turbulent flow over a flat plate, and all another parameter as in the expression (4.25), thus

$$k = 0.41, I_0^+ = 8.71, g_y^+ = -g_x^+ \cos a_0 / \sin a_0, z_0 = H / 2, V_* = 0.27.$$

The difference in the determination of the mixing layer parameter z_0 for the wind velocity components can be explained, first of all, by the fact that the turbulent flow in the atmospheric surface layer varies with time so that the acceleration due to the daily wind velocity variations, $\partial U_0 / \partial t$, approximately equals to the acceleration due to the planet rotation, $2\Omega_z U_0$. Therefore, the wind velocity profile is the fragment of a solution dependent on time.

The second reason is that the linear form of the equation system (2.12) has been used, to derive the mean velocity component profiles (4.25)-(4.26), as follows (see also [47])

$$(1+x^2) \frac{d^2 j}{dx^2} + 2x \frac{dj}{dx} = \frac{I^+ a_{out} p_1}{1+x^2} \quad (4.27)$$

$$(1+x^2) \frac{d^2 y}{dx^2} + x \frac{dy}{dx} = I^+ a_{out} p_2$$

where $x = (z - z_0) / V_* H$, $I^+ = V_* H n / u_*$, a_{out} is the pressure parameter in the outer region,

$$p_1 = \frac{I^+ n}{r u_*^3} \left(\frac{\mathcal{I} p}{\mathcal{I} x} \cos a + \frac{\mathcal{I} p}{\mathcal{I} y} \sin a \right), \quad p_2 = \frac{I^+ n}{r u_*^3} \left(\frac{\mathcal{I} p}{\mathcal{I} x} \sin a - \frac{\mathcal{I} p}{\mathcal{I} y} \cos a \right).$$

The equation system (4.27) can be integrated in common case as

$$j = j_0 + j_1 \arctan x + \frac{I^+ a_{out} p_1}{2} \arctan^2 x \tag{4.28}$$

$$y = y_0 + y_1 \operatorname{Arsh} x + \frac{I^+ a_{out} p_2}{2} \operatorname{Arsh}^2 x$$

where j_i, y_i are constants which can be calculated from the inner layer problem. This solution has been used to recover the profiles (4.25) - (4.26) in the upper layer. Hence, as follows from (4.27), the real Coriolis forces has been replaced by the pressure gradient effect.

Nevertheless the model (4.25)-(4.26) can be used for the wind profile estimation in the atmospheric boundary layer. The mean velocity profile and the turning of wind with height computed on the model (4.25)-(4.26) are shown in Figure 4.9 - the solid lines, in comparison with the Leipzig data - the black points. The turning angle and the wind velocity are defined as follows $\bar{\alpha} = \arctan(v/u)$, $U = \sqrt{u^2 + v^2}$.

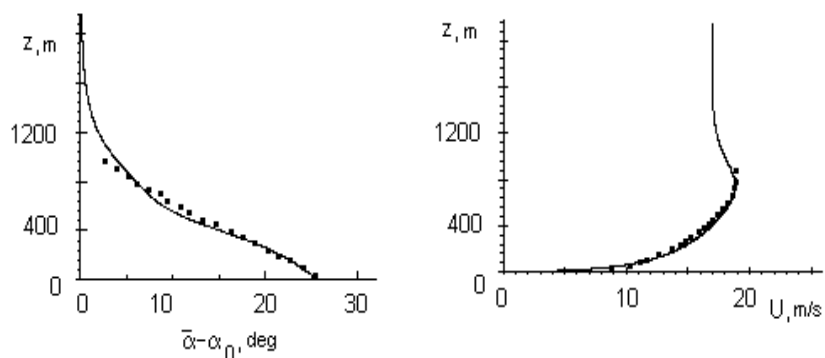


Figure 4.9: Turning of wind with height (left) and the wind velocity profile (right) in the neutral stratified atmospheric boundary layer computed on (4.25)-(4.26) - the solid lines, and the Leipzig experimental data [125]

As it has been established, the computed profiles depend on the "infinite" point in which the values u_∞^+, v_∞^+ are defined. The best correlation with the Leipzig data has been obtained for $z_\infty = 3000_M$. This upper bound has also been used for the atmospheric boundary layer parameters estimation by Apsley & Castro

[44]. This dependence means that the atmospheric boundary layer can be influenced by the upper layer in a common case including the neutral stratification.

(To be continued)

References

- [1] Liepmann, H.W., The Rise and Fall of Ideas in Turbulence, *American Scientist*, **67**, pp. 221-228, 1979.
- [2] Amirkhanov, M.M, Lukashina, N.S. & Trunev, A. P., *Natural recreation resources, state of environment and economical and legal status of coastal resorts*, Publishing House "Economics", Moscow, 207 p., 1997 (in Russian).
- [3] Marchuk, G. I., *Mathematical Modelling in the Environmental Problem*, "Nauka", Moscow, 1982 (in Russian).
- [4] Borrell P.M., Borrell P., Cvitas T. & Seiler W., Transport and transformation of pollutants in the troposphere. *Proc. EUROTRAC Symp.*, SPB Academic Publishing, Hague, 1994.
- [5] Jaecker-Voirol A., Lipphardt M., Martin B., Quandalle, Ph., Salles, J., Carissimo, B., Dupont, E., Musson-Genon, L., Riboud, P.M., Aumont, B., Bergametti, G., Bey, I., Toupance, G., A 3D regional scale photochemical air quality model - application to a 3 day summertime episode over Paris, *Air Pollution IV. Monitoring, Simulation and Control*, eds. B. Caussade, H. Power & C.A. Brebbia, Comp. Mech. Pub., Southampton, pp. 175-194, 1996.
- [6] Borrego, C., Coutinho, M., Carvalho, A.C.& Lemos, S., A modelling package for air quality management in Lisbon, *Air Pollution V. Modelling, Monitoring and Management*, eds. H. Power, T. Tirabassi & C.A. Brebbia, CMP, Southampton-Boston, pp. 35-44, 1997.
- [7] Bozo, L.& Baranka, G., Air quality modelling over Budapest, *Air Pollution IV. Monitoring, Simulation and Control*, eds. B. Caussade, H. Power & C.A. Brebbia, Comp. Mech. Pub., Southampton, pp. 31-36, 1996.
- [8] Marchuk, G.I. & Aloyan, A.E., Global Admixture Transport in the Atmosphere, *Proc. Rus. Acad. Sci., Phys. Atmosphere and Ocean*, **31**, pp. 597-606, 1995.
- [9] Moussiopoulos N., Air pollution models as tools to integrate scientific results in environmental policy, *Air Pollution III, Vol.1. Theory and Simulation*, eds. H. Power, N. Moussiopoulos & C.A. Brebbia, Comp. Mech. Publ., Southampton, pp.11-18, 1995.
- [10] Pekar M., *Regional models LPMOD and ASIMD. Algorithms, parametrization and results of application to Pb and Cd in Europe scale for 1990*, EMEP/MSC-E Report 9/96, Aug, 78 p., 1996.
- [11] Carruthers, D.J, Edmunds, H.A., McHugh, C.A., Riches, P.J. & Singles, R.J., ADMS Urban - an integrated air quality modelling system for local government, *Air Pollution V. Modelling, Monitoring and Management*, eds. H. Power, T. Tirabassi & C.A. Brebbia, CMP, Southampton-Boston, pp. 45-58, 1997.
- [12] Ni Riain, C., Fisher, B., Martin, C. J. & Littler J., Flow field and Pollution Dispersion in a Central London Street, *Proc. of the 1st Int. Conf. on Urban Air Quality: Monitoring and Modelling*, ed. R. S. Sokhi, Kluwer Academic Publishers, pp. 299-314, 1998.
- [13] Lukashina, N.S. & Trunev, A. P., *Principles of Recreation Ecology and Natural Economics*, Russian Academy of Sciences, Sochi, 273 p., 1999 (in Russian).
- [14] Lukashina, N.S., Amirkhanov, M.M, Anisimov, V.I. & Trunev, A.P., Tourism and environmental degradation in Sochi, Russia, *Annals of Tourism Research*, **23**, pp. 654-665, 1996.
- [15] Lenhart, L. & Friedrich, R. European emission data with high temporal and spatial resolution, *Air Pollution III Vol.2: Air Pollution Engineering and management*, eds. H. Power, N. Moussiopoulos & C.A. Brebbia. Comp. Mech. Pub., Southampton, pp.285-292, 1995.
- [16] Oke, T.R., Street design and urban canopy layer climate, *Energy and Buildings*, **11**, pp. 103-111, 1988.

- [17] Zilitinkevich, S. Non-local turbulent transport: pollution dispersion aspects of coherent structure of convective flows, *Air Pollution III*, Vol.1. *Air Pollution Theory and Simulation*, eds. H. Power, N. Moussiopoulos & C.A.Brebbia, Comp. Mech. Publ., Southampton, pp.-53-60, 1995.
- [18] Arya, S. P., *Introduction to Micrometeorology*, Academic Press, San Diego, 307 p., 1988.
- [19] Stull, R. B., *An Introduction to Boundary Layer Meteorology*, Kluwer Academic Publishers, Dordrecht, 666 p., 1988.
- [20] Kaimal, J. C. & Finnigan, J. J., *Atmospheric Boundary Layer Flows: Their Structure and Measurements*, Oxford University Press, 289 p., 1994.
- [21] Monin, A.S. & Obukhov, A.M., Basic Laws of Turbulent Mixing in the Atmospheric surface layer, *Trudy Geofiz. Inst. Akad. Nauk SSSR* **24** (151), pp. 163-187, 1954.
- [22] Monin, A. S., The Atmospheric Boundary Layer, *Ann. Rev. Fluid Mech.*, **22**, 1970.
- [23] Businger, J.A., Wyngaard, J.C., Izumi, Y. & Bradley, E.F. Flux Profile Relationships in the Atmospheric Surface Layer, *J. Atmos. Sciences*, **28**, pp.181-189, 1971.
- [24] Businger, J. A., A Note on the Businger-Dyer Profile, *Boundary-Layer Meteorol.*, **42**, pp. 145–151, 1988.
- [25] Yaglom, A.M., Data on Turbulence Characteristics in the Atmospheric Surface Layer, *Izv. Acad. Sci. USSR, Phys. Atmosphere and Ocean*, **10**, pp. 566-586, 1974.
- [26] Dyer, A. J., A Review of Flux-Profile Relationships, *Boundary-Layer Meteorol.*, **7**, pp. 363–372, 1974.
- [27] Van Ulden, A. & Holtslag, A. A. M., Estimation of Atmospheric Boundary Layer Parameters for Diffusion Applications, *J. Clim. Appl. Meteorol.*, **24**, pp. 1196–1207, 1985.
- [28] Hanjalic, K. & Launder, B. E., A Reynolds Stress Model of Turbulence and its Application to Thin Shear Flows, *J. Fluid Mech*, **52**, pp. 609–638, 1972.
- [29] Rodi, W. Calculation of Stably Stratified Shear-layer Flows with a Buoyancy-extended $k - \epsilon$ Turbulence Model, *Turbulence and Diffusion in Stable Environments*, ed. J. C. R. Hunt, Clarendon Press, Oxford, pp. 111–143, 1985.
- [30] Mellor, G. L. & Yamada, T. A, Hierarchy of Turbulence Closure Models for Planetary Boundary Layers, *J. Atmos. Sci.*, **31**, pp. 1792–1806, 1974.
- [31] Mellor, G. L. & Yamada, T., Development of a Turbulence Closure Model for Geophysical Fluid Problems, *Rev. Geophys. Space Phys.*, **20**, pp.851–875, 1982.
- [32] Wyngaard, J. C. & Cote, O. R., The Evolution of a Convective Planetary Boundary Layer – a Higher-order-closure Model Study, *Boundary-Layer Meteorol.*, **7**, pp. 289–308, 1974.
- [33] Zeman, O. & Lumley, J. L., Modelling Buoyancy Driven Mixed Layers, *J. Atmos. Sci.*, **33**, pp.1974–1988, 1976.
- [34] Deardorff, J. W. & Willis, G. E., Further Results from a Laboratory Model of the Convective Boundary Layer, *Boundary-Layer Meteorol*, **32**, pp. 205–236, 1985.
- [35] Enger, L., A Higher Order Closure Model Applied to Dispersion in a Convective PBL, *Atmos. Environ.*, **20**, pp. 879–894, 1986.
- [36] Holt, T. & Raman, S., A Review and Comparative Evaluation of Multilevel Boundary Layer Parameterisations for First Order and Turbulent Kinetic Energy Closure Schemes, *Rev. Geophys. Space Phys.*, **26**, pp. 761–780, 1988.
- [37] Danilov, S.D., Koprov, B. M. & Sazonov, L. A., Atmospheric Boundary Layer and the Problem of Its Description (Review), *Proc. Rus. Acad. Sci., Phys. Atmosphere and Ocean*, **31**, pp. 187–204, 1995.
- [38] Hurley, P. J., An Evaluation of Several Turbulence Schemes for the Prediction of Mean and Turbulent Fields in Complex Terrain, *Boundary-Layer Meteorol.*, **83**, pp. 43–73, 1997.
- [39] Reynolds, O., On the dynamically theory of incompressible viscous fluids and the determination of the criterion, *Philos. Trans. R. Soc. London*, **A 186**, 123, 1895.
- [40] Boussinesq, J., Theorie de l'ecoulement tourbillant, *Mem. Pres. Acad. Sci.*, **23**, p. 46, 1877.
- [41] Prandtl, L., Bericht uber untersuchungen zur ausgebildeten turbulenz, *Z. Angew. Math. Mech.*, **5**, pp.136-139, 1925.
- [42] Prandtl, L., Neuere Ergebnisse der Turbulenzforschung, *VDI -Ztschr.*, **77**, 5, p.105, 1933.
- [43] Kolmogorov, A.N., The Equations of Turbulent Motion in an Incompressible Fluid, *Izv. Acad. Sci. USSR, Phys.*, **6**, pp. 56-58, 1942.

- [44] Apsley, D. D. & Castro, I. P., A Limited-Length-Scale-Model for the Neutral and Stable-Stratified Atmospheric Boundary Layer, *Boundary Layer Meteorol.*, **83**, pp. 75–98, 1997.
- [45] Trunev, A. P., Diffuse processed in turbulent boundary layer over rough surface, *Air Pollution III, Vol.1. Theory and Simulation*, eds. H. Power, N. Moussiopoulos & C.A. Brebbia, Comp. Mech. Publ., Southampton, pp. 69-76, 1995.
- [46] Trunev, A. P., Similarity theory and model of turbulent dusty gas flow over large-scale roughness, *Abstr. of Int. Conf. On Urban Air Quality: Monitoring and Modelling*, University of Hertfordshire, Institute of Physics, London, p. 3.8, 1996.
- [47] Trunev, A. P., Similarity theory for turbulent flow over natural rough surface in pressure and temperature gradients, *Air Pollution IV. Monitoring, Simulation and Control*, eds. B. Caussade, H. Power & C.A. Brebbia, Comp. Mech. Pub., Southampton, pp. 275-286, 1996.
- [48] Trunev, A. P., Similarity theory and model of diffusion in turbulent atmosphere at large scales, *Air Pollution V. Modelling, Monitoring and Management*, eds. H. Power, T. Tirabassi & C.A. Brebbia, CMP, Southampton-Boston, pp. 109-118, 1997.
- [49] Klebanoff, P. S., Characteristics of turbulence in a boundary layer with zero pressure gradient, *NACA Tech. Note*, **3178**, 1954.
- [50] Laufer, J., The structure of turbulence in fully developed pipe flow, *NACA Tech. Note*, **2954**, 1954.
- [51] Cebeci, T. & Bradshaw, P., *Physical and Computational Aspects of Convective Heat Transfer*, Springer-Verlag, NY, 1984.
- [52] Cantwell, Brian J., Organized motion in turbulent flow, *Ann. Rev. Fluid Mech.*, **13**, pp. 457-515, 1981.
- [53] Kuroda, A., *Direct Numerical Simulation of Couette-Poiseuille Flows*, Dr. Eng. Thesis, the University of Tokyo, Tokyo, 1990.
- [54] Coleman, G.N., Ferziger, J. R. & Spalart, P. R., A numerical study of the turbulent Ekman layer, *J. Fluid Mech.*, **213**, pp.313-348, 1990.
- [55] Trunev, A. P. & Fomin, V. M., Continual model of impingement erosion, *J. Applied Mech. Tech. Phys.*, **6**, pp. 113-120, 1985.
- [56] Trunev, A. P., *Research of bodies erosion distraction in gas flows with admixture particles*, Ph.D. Thesis, Inst. Theoretical and Appl. Mech., Novosibirsk, 1986.
- [57] Nikolaevskii, V.N., The space averaging in the turbulence theory, *Vortexes and Waves*, ed. V.N. Nikolaevskii, Mir, Moscow, pp. 266-335, 1984 (in Russian).
- [58] Landau, L.D. & Lifshitz, E. M., *Hydrodynamics*, 3rd ed., Nauka, Moscow, 1986 (in Russian).
- [59] Pulliam, T. H. & Steger, J. L., Implicit Finite-Difference Simulations of three-dimensional Compressible Flow, *AIAA Journal*, **18**, p. 159, 1980.
- [60] Hirschel, E.H. & Kordulla, W., *Shear Flow in Surface-Oriented Coordinates*, Friedr. Vieweg & Sohn, Wiesbaden, 1986.
- [61] Schlichting, H., *Boundary Layer Theory*, McGraw-Hill, NY, 1960.
- [62] Kutateladze, S.S., *The Wall Turbulence*, Nauka, Novosibirsk, 1973 (in Russian).
- [63] Hairer, E., Norsett, S.P. & Wanner, G., *Solving Ordinary Differential Equations 1. Nonstiff Problems*, Springer-Verlag, Berlin, 1987.
- [64] Cantwell, B. J., Coles, D. E. & Dimotakis, P. E., Structure and entrainment in the plane of symmetry of a turbulent spot, *J. Fluid Mech.*, **87**, pp. 641-672, 1978.
- [65] Van Driest, E.R., On turbulent flow near a wall, *J. Aero. Sci.*, **23**, p.1007, 1956.
- [66] Kuroda, A., Kasagi, N. & Hirata, M., A Direct Numerical Simulation of the Fully Developed Turbulent Channel Flow, *Proc. Int. Symp. on Computational Fluid Dynamics*, Nagoya, pp. 1174-1179, 1989.
- [67] Nagano, Y., Tagawa, M. & Tsuji, T., Effects of Adverse Pressure Gradients on Mean Flows and Turbulence Statistics in a Boundary Layer, *Proc. 8th Symposium on Turbulent Shear Flows*, 1992.
- [68] Nagano, Y., Kasagi, N., Ota, T., Fujita, H., Yoshida, H. & Kumada, M., *Data-Base on Turbulent Heat Transfer*, Department of Mechanical Engineering, Nagoya Institute of Technology, Nagoya, DATA No. FW BL004, 1992.
- [69] Smith, R.W., *Effect of Reynolds Number on the Structure of Turbulent Boundary Layers*, Ph.D. Thesis, Princeton University, Princeton, NJ, 1994.

- [70] Kline, S.J., Reynolds, W.C., Schraub, F.A. & Runstadler P.W., The structure of turbulent boundary layers, *J. Fluid Mech.*, **30**, pp. 741-773, 1967.
- [71] Kriklivy, V.V., Trunev, A.P. & Fomin, V.M., Investigation of two-phase flow in channel with damaging wall, *J. Applied Mech. Tech. Phys.*, **1**, pp. 82-87, 1985.
- [72] Trunev, A. P. & Fomin, V.M., Surface instability during erosion in the gas-particles stream, *J. Applied Mech. Tech. Phys.*, **3**, pp. 78-84, 1986.
- [73] Trunev, A. P., Evolution of the surface relief at sputtering by ionic bombardment, *Interaction of nuclear particles with a rigid body*, Moscow, Vol.1, Part 1, pp. 83-85, 1989.
- [74] Blackwelder, R. F. & Eckelmann, H., Streamwise vortices associated with the bursting phenomena, *J. Fluid Mech.*, **94**, pp. 577-594, 1979.
- [75] Nikuradse, J., Strömungsgesetze in Rauhen Röhren, *ForschHft. Ver. Dt. Ing.*, p. 361, 1933.
- [76] Schlichting, H., Experimentelle Untersuchungen zum Rauheitsproblem, *Ing.-Arch*, **7**(1), pp.1-34, 1936.
- [77] Bettermann, D., Contribution a l'Etude de la Convection Force Turbulente le Long de Plaques Regueuses, *Int. J. Heat and Mass Transfer*, **9**, p. 153, 1966.
- [78] Millionschikov, M.D., *Turbulent flows in the boundary layer and in the tubes*, Nauka, Moscow, 1969 (in Russian).
- [79] Dvorak, F. A., Calculation of Turbulent Boundary Layer on Rough Surface in Pressure Gradient, *AIAA Journal*, **7**, 1969.
- [80] Dirling, R.B., Jr., A Method for Computing Roughwall Heat-Transfer Rate on Re-Entry Nose Tips, *AIAA Paper*, **73-763**, 1973.
- [81] Simpson, R. L., A Generalized Correlation of Roughness Density Effect on the Turbulent Boundary Layer, *AIAA Journal*, **11**, pp. 242-244, 1973.
- [82] Donne, M. & Meyer, L., Turbulent Convective Heat Transfer from Rough Surfaces with Two-Dimensional Rectangular Ribs, *Int. J. Heat Mass Transfer*, **20**, pp. 583-620, 1977.
- [83] Coleman, H. W., Hodge, B. K. & Taylor, R. P., A Reevaluation of Schlichting's Surface Roughness Experiment, *J. Fluid Eng.*, **106**, pp. 60-65, 1984.
- [84] Clauser, F., The Turbulent Boundary Layer, *Advances in Applied Mechanics*, **4**, pp.1-51, 1956
- [85] Grabov, R. M. & White, C. O., Surface Roughness Effects on Nose Tip Ablation Characteristics, *AIAA Journal*, **13**, pp. 605-609, 1975.
- [86] Sigal, A. & Danberg, J. E., New Correlation of Roughness Density Effect on the Turbulent Boundary Layer, *AIAA Journal*, **25**, pp.554-556, 1990.
- [87] Kind, R. J. & Lawrysyn, M. A., Aerodynamic Characteristics of Hoar Frost Roughness, *AIAA Journal*, **30**, pp. 1703-7, 1992.
- [88] Gargaud, I. & Paumard, G., *Amelioration du transfer de chaleur par l'emploi de surfaces corruees*, CEA-R-2464, 1964.
- [89] Draycott, A. & Lawther, K.R., Improvement of fuel element heat transfer by use of roughened surface and the application to a 7-rod cluster, *Int. Dev. Heat Transfer*, Part III, pp. 543-52, ASME, NY. 1961.
- [90] Möbius, H., Experimentelle Untersuchung des Widerstandes und der Gschwindigkeitsverteilung in Röhren mit regelmäßig angeordneten Rauigkeiten bei turbulenter Strömung, *Phys. Z.*, **41**, pp. 202-225, 1940
- [91] Chu, H. & Streeter, V.L., *Fluid flow and heat transfer in artificially roughened pipes*, Illinois Inst. of Tech. Proc., No. 4918, 1949.
- [92] Koch, R., Druckverlust und Wärmeübergang bei verwirbelter Strömung, *ForschHft. Ver. Dt. Ing.*, Series B, **24**, pp. 1-44, 1958.
- [93] Skupinski, E., *Wärmeübergang und Druckverlust bei künstlicher Verwirbelung und künstlicher Wandrauigkeiten*, Diss. Techn. Hochschule, Aachen, 1961.
- [94] Webb, R. L., Eckert, E.R.G. & Goldstein, R. J., Heat transfer and friction in tubes with repeated-rib roughness, *Int. J. Heat Mass Transfer*, **14**, pp. 601-617, 1971.
- [95] Fuerstein, G. & Rampf, G., Der Einfluß rechteckiger Rauigkeiten auf den Wärmeübergang und den Druckabfall in turbulenter Ringspaltströmung, *Wärme- und Stoffübertragung*, **2** (1), pp.19-30, 1969.
- [96] Sams, E.W., *Experimental investigation of average heat transfer and friction coefficients for air flowing in circular tubes having square-thread-type roughness*, NACA RME 52 D 17, 1952.

- [97] Fedynskii, O. S., Intensification of heat transfer to water in annular channel, *Problemi Energetiki, Energ. Inst. Akad. Nauk USSR*, 1959 (in Russian).
- [98] Watson, M.A.P., *The performance of a square rib type of heat transfer surface*, CEGB RD/B/N 1738, Berkeley Nuclear Laboratories, 1970.
- [99] Kjellström, B. & Larsson, A. E., *Improvement of reactor fuel element heat transfer by surface roughness*, AE-271, 1967, Data reported by Dalle Donne & Meyer (1977).
- [100] Savage, D.W. & Myers, J.E., The effect of artificial surface roughness on heat and momentum transfer, *A.I.Ch.E.J.*, **9**, pp.694-702, 1963.
- [101] Sheriff, N., Gumley, P. & France, J., *Heat transfer characteristics of roughened surfaces*, UKAEA, TRG Report 447 (R), 1963.
- [102] Massey, F.A., *Heat transfer and flow in annuli having artificially roughened inner surfaces*, Ph. D. Thesis, University of Wisconsin, 1966.
- [103] Nunner, W., Wärmeübergang und Druckabfall in rauhen Röhren, *ForschHft. Ver. Dt. Ing.*, p. 455, 1956.
- [104] Lawn, C. J. & Hamlin, M. J., *Velocity measurements in roughened annuli*, CEGB RD/B/N 2404, Berkeley Nuclear Laboratories, 1969
- [105] Stephens, M. J., *Investigations of flow in a concentric annulus with smooth outer wall and rough inner wall*, CEGB RD/B/N 1535, Berkeley Nuclear Laboratories, 1970.
- [106] Perry, A.E. & Joubert, P.N., Rough-Wall Boundary Layers in Adverse Pressure Gradients, *J. Fluid Mech.*, **17**, pp.193-211, 1963.
- [107] Antonia, R.A. & Luxton, R.E., The Response of a Turbulent Boundary Layer to a Step Change in Surface Roughness, Pt. 1. Smooth to Rough, *J. Fluid Mech.*, **48**, pp. 721-762, 1971
- [108] Antonia, R.A. & Wood, D.H., Calculation of a Turbulent Boundary layer Downstream of a Step Change in Surface Roughness, *Aeronautical Quarterly*, **26**, pp. 202-210, 1975.
- [109] Pineau, F., Nguyen, V. D., Dickinson, J. & Belanger, J., Study of a Flow Over a Rough Surface with Passive Boundary-Layer Manipulators and Direct Wall Drag Measurements, *AIAA Paper*, **87-0357**, 1987.
- [110] Osaka, H. & Mochizuki, S., Mean Flow Properties of a d-type Rough Wall Boundary Layer in a Transitionally Rough and a Fully Rough Regime, *Trans. JSME ser. B*, **55**, pp. 640-647, 1989.
- [111] Byzova, N.L., Ivanov, V.N. & Garger, E.K., *Turbulence in the Atmospheric Boundary Layer*, Leningrad, Hydrometeoizdat, 1989 (in Russian).
- [112] Jackson, P.S., On the displacement height in the logarithmic wind profile. *J. Fluid Mech.*, **111**, pp. 15-25, 1981.
- [113] Wieringa, J., Updating the Davenport Roughness Clarification. *J. Wind Engineer, Industl. Aerodyn*, **41**, pp. 357-368, 1992.
- [114] Bottema, M., Parameterization of aerodynamic roughness parameters in relation with air pollutant removal efficiency of streets, *Air Pollution III, Vol.2. Air Pollution Engineering and Management*, eds. H. Power, N. Moussiopoulos & C. A. Brebbia, Comp. Mech. Publ., Southampton, pp. 235-242, 1995.
- [115] Kutateladze, S. S., *Similarity Analysis in the Thermal-physics*, Novosibirsk, Nauka, 1982 (in Russian).
- [116] Kim, J., Investigation of Heat and Mass Transport in Turbulent Flows via Numerical Simulation, *Transport Phenomena in Turbulent Flows: Theory, Experiment and Numerical Simulation*, eds. M. Hirata & N. Kasagi, Hemisphere Publishing Corp., Washington, D. C., pp. 157-170, 1988.
- [117] Hogstrom, U., Review of Some Basic Characteristics of the Atmosphere Surface Layer, *Boundary-Layer Meteorol.*, **78**, pp. 215-246, 1996.
- [118] Beljaars, A. C. M. & Holtslag, A. A. M., Flux Parameterization over Land Surfaces for Atmospheric Models, *J. Appl. Meteorol.*, **30**, pp. 327-341, 1991.
- [119] Pugliese, S., Jaeger, M. & Occelli, R., Finite element modelling of plume dispersion in the lower part of the atmosphere, *Air Pollution IV. Monitoring, Simulation and Control*, eds. B. Caussade, H. Power & C.A. Brebbia, Comp. Mech. Pub. Southampton-Boston, 99-108, 1996
- [120] Lui, Jingmiao & Kotoda, Kazuo, Evaluation of Surface-Layer Wind Profiles With Heife Observations, *Boundary-Layer Meteorol.*, **83**, pp. 27-41, 1997.
- [121] Castillo, L., *Similarity analysis of turbulent boundary layers*, Ph. D. Thesis, The Graduate School of the State University of New York, Buffalo, 1997.

- [122] Clauser, F.H., Turbulent boundary layer in adverse pressure gradients, *J. Aeron. Sci.*, **21**, pp. 91-108, 1954.
- [123] Herring, H. & Norbury, J., Some experiments on equilibrium turbulent boundary layers in favourable pressure gradients, *J. Fluid mech.*, **27**, pp. 541-549, 1967.
- [124] Patel, V.C. & Head, M.R., Reversion of Turbulent to Laminar Flow, *J. Fluid. Mech.*, **34**, pp. 371-392, 1968.
- [125] Detering, H. W. & Etling, D., Application of the E- ϵ Turbulence Model to the Atmospheric Boundary Layer, *Boundary-Layer Meteorol*, **33**, pp. 113–133, 1985.